RR LYRAE STARS IN GALACTIC GLOBULAR CLUSTERS. III. PULSATIONAL PREDICTIONS FOR METAL CONTENT $Z = 0.0001$ TO $Z = 0.006$

M. DI CRISCIENZO,[1,2] M. MARCONI,[1] AND F. CAPUTO[3]
Received 2004 January 13; accepted 2004 May 19

ABSTRACT

The results of nonlinear, convective models of RR Lyrae pulsators with metal content $Z = 0.0001 - 0.006$ are discussed and several predicted relations connecting pulsational (period and amplitude of pulsation) and evolutionary parameters (mass, absolute magnitude, and color of the pulsator) are derived. These relations, when linked with the average mass of RR Lyrae stars, as suggested by horizontal-branch evolutionary models, provide a "pulsational" route to the determination of the distance modulus, both apparent and intrinsic, of RR Lyrae–rich globular clusters. Based on a preliminary set of synthetic horizontal-branch simulations, we compare the predicted relations with observed variables in selected globular clusters (M2, M3, M5, M15, M55, M68, NGC 1851, NGC 3201, NGC 5466, NGC 6362, NGC 6934, and IC 4499). We show that the distance moduli inferred by the various theoretical relations are mutually consistent within the errors, provided that the value of the mixing-length parameter slightly increases from the blue to the red edge of the pulsation region. Moreover, we show that the relative "pulsational" distance moduli fit well previous empirical results and that the parallax of the prototype variable RR Lyr, as inferred by the predicted period-Wesenheit relation, is in close agreement with the *Hubble Space Telescope* astrometric measurement.

Subject headings: globular clusters: general — stars: evolution — stars: horizontal-branch — stars: variables: other

1. INTRODUCTION

RR Lyrae stars represent the most common type of Population II radially pulsating stars, with approximately 3000 variables in Galactic globular clusters (see Clement et al. 2001) and increasing samples being discovered in all Local Group galaxies. If members of globular clusters (GCs), they show low ($Z \sim 0.0001$) to intermediate metal content ($Z \leq 0.006$), but up to solar abundances are measured for field variables. They represent fundamental tracers of ancient stellar populations and, via the calibration of their absolute visual magnitude $M_V(\mathrm{RR})$ in terms of the measured iron-to-hydrogen content [Fe/H], they are commonly used as standard candles for distance determinations in the Local Group, with relevant implications for the cosmic distance scale and the age of globular clusters (see e.g. Carretta et al. 2000; Cacciari 2003). For these reasons, several observational and theoretical efforts have been made in the last years to provide accurate evaluations of the $M_V(\mathrm{RR})$ versus [Fe/H] relation, which is commonly approximated in the linear form $M_V(\mathrm{RR}) = \alpha + \beta[\mathrm{Fe/H}]$.

Although the discussion of the $M_V(\mathrm{RR})$-[Fe/H] relation is beyond the purpose of the present paper, it is worth mentioning that, from the side of empirical studies, recent evaluations of the zero-point α are spanning an interval of about 0.3 mag, while the value of the slope β ranges from $\sim$0.13 to $\sim$0.30 mag dex^{-1}. As an example, according to the very recent review by Cacciari (2003), the value of $M_V(\mathrm{RR})$ at $[\mathrm{Fe/H}] = -1.5$ varies from 0.56 ± 0.15 mag ("revised" Baade-Wesselink method) and 0.62 ± 0.10 mag (direct astrometry to GCs) to 0.68 ± 0.08 mag

("classical" Baade-Wesselink method) and 0.77 ± 0.13 mag (statistical parallaxes). Concerning the theoretical approach, we have already discussed (Marconi et al. 2003, hereafter Paper II) that the predicted $M_V(\mathrm{RR})$-[Fe/H] relation inferred by horizontal branch (HB) evolutionary models depends on several factors (e.g., the color distribution of HB stars, the adopted ratio between α- and heavy elements, the adopted bolometric correction), and it should be handled with care, also in consideration of the fact that HB models yield "static" magnitudes (i.e. the values the star would have were it not pulsating), whereas observed magnitudes are "mean" quantities averaged over the pulsation cycle, which not necessarily are exactly alike static values.

In summary, in spite of a huge amount of work, we are presently facing a quite intriguing scenario: on the evolutionary side, even for a fixed dependence of the luminosity $L(\mathrm{RR})$ on Z, the predicted $M_V(\mathrm{RR})$-[Fe/H] relation turns out to depend on several assumptions (bolometric correction, [α/Fe] ratio, evolutionary status of the variables), while on the observational side no firm evaluation has been reached yet. Note that even the recent *Hubble Space Telescope* (*HST*) determination of a quite accurate trigonometric parallax ($\pi_{\mathrm{trig}} = 3.82 \pm 0.20$ mas) for the prototype variable RR Lyr ($[\mathrm{Fe/H}] = -1.39$) yields $M_V = 0.607 \pm 0.114$ mag ± 0.034 mag, where the last two figures illustrate, respectively, the intrinsic uncertainty of the *HST* measurement and the effect of an interstellar extinction $A(V) = 0.087 \pm 0.034$ mag (see Benedict et al. 2002; Bono et al. 2003).

In this context, the study of quantities such as the pulsation period and amplitude is of fundamental importance since they depend on the star structural parameters (mass, luminosity, and effective temperature) and are distance- and reddening-free observable quantities as well. In order to perform a thorough analysis of observed RR Lyrae stars (see Castellani et al. 2003 [Paper I] for the observational scenario of these variables in Galactic GCs), we planned to construct a theoretical framework based on both pulsation and evolution models computed at various metal content and using the same input physics. The

[1] INAF–Osservatorio Astronomico di Capodimonte, via Moiarello 16, I-80131 Napoli, Italy; marcella@na.astro.it, dicrisci@na.astro.it.
[2] Universita "Tor Vergata," via della Ricerca Scientifica 1, I-00133, Rome, Italy.
[3] INAF–Osservatorio Astronomico di Roma, Via di Frascati, 33, I-00040 Monte Porzio Catone Italy; caputo@mporzio.astro.it.

TABLE 1
Stellar Parameters for the Full Set of Pulsation Models

Y	Z	$M/M_\odot$	$\log L/L_\odot$
0.24...........................	0.0001	0.80	1.72, 1.81, 1.91
		0.75	1.61, 1.72, 1.81
		0.70	1.72
		0.65	1.61
0.24...........................	0.0004	0.70	1.61, 1.72, 1.81
0.24...........................	0.001	0.75	1.71
		0.65	1.51, 1.61, 1.72
0.255.........................	0.006	0.58	1.55, 1.65, 1.75

Notes.—All the computations, except those with $Z = 0.0004$, adopt $l/H_p = 1.5$ and 2.0.

general procedure has been discussed in detail in Paper II, where the results at $Z = 0.001$, the typical metal content of Oosterhoff type I clusters, are compared with RR Lyrae stars in M3. In the present paper, we discuss nonlinear convective pulsation models for $Z = 0.0001$, 0.0004, and 0.006, while an extensive atlas of synthetic HB computations will be given in a future paper (S. Cassisi et al. 2004, in preparation [Paper IV]).

Following the organization of Paper II, we present in § 2 the pulsation models and the relevant relations among the various parameters, while a first comparison with observed variables in RR Lyrae–rich globular clusters is given in § 3. Some brief remarks close the paper.

2. THE THEORETICAL PULSATIONAL SCENARIO

2.1. Periods, Magnitudes, and Colors

The existing grid of nonlinear and convective models, as computed with a mixing length parameter $l/H_p = 1.5$ (see Bono et al. 2001, 2003 and Paper II), has been extended to new fundamental (F) and first-overtone (FO) computations with $Z = 0.0001$, adopting mass $M = 0.80 \ M_\odot$ and $\log L/L_\odot = 1.72$, 1.81, 1.91 (Di Criscienzo 2002) and $M = 0.65 \ M_\odot$ and $\log L/L_\odot = 1.61$ (present paper). As a result, we are dealing with the set of pulsation models listed in Table 1. The bolo-

TABLE 2
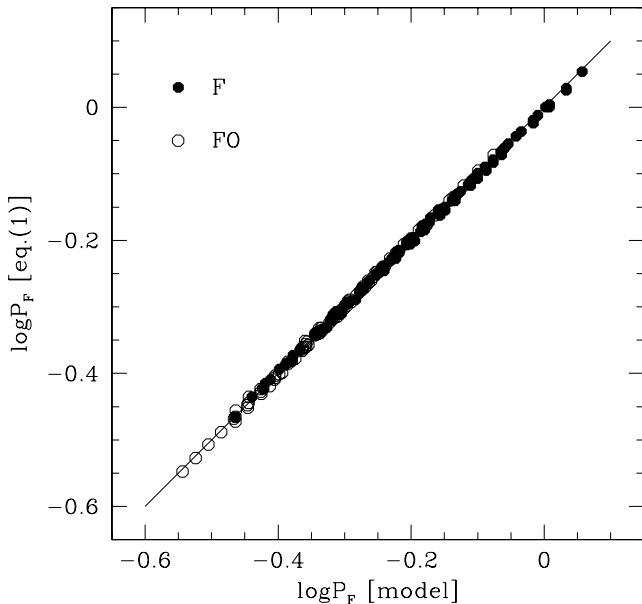Predicted Period-Magnitude-Color Relation $\log P'_F = a + b[\langle M_B \rangle - \langle M_V \rangle]$ with Intensity-averaged BV Magnitudes

Z	a	b
0.0001...........................	-0.552 ± 0.014	1.290 ± 0.029
0.0004...........................	-0.543 ± 0.014	1.256 ± 0.029
0.001...........................	-0.545 ± 0.014	1.208 ± 0.028
0.006...........................	-0.522 ± 0.018	1.019 ± 0.029

metric light curves of all these models have been transformed into the observational plane by adopting the bolometric corrections and temperature-color transformations provided by Castelli et al. (1997a, 1997b, hereafter CGKa and CGKb). In this way, light-curve amplitudes and mean absolute magnitudes, either intensity-weighted $\langle M_i \rangle$ or magnitude-weighted (M_i), are derived in the various photometric bands.

As a first step we investigated the dependence, if any, of the pulsation-period relation $P = f(M, L, T_e)$ on the metal content. After confirming that the period of FO pulsators can be fundamentalized adopting $\log P_F = \log P_{FO} + 0.130 \pm 0.004$, we derive (see Fig. 1) that all over the explored range of mass, luminosity, and metal content, the pulsation equation can be approximated as

$$\log P_F = 11.038(\pm 0.003) + 0.833(\pm 0.003) \log L/L_\odot$$
$$- 0.651(\pm 0.007) \log M/M_\odot$$
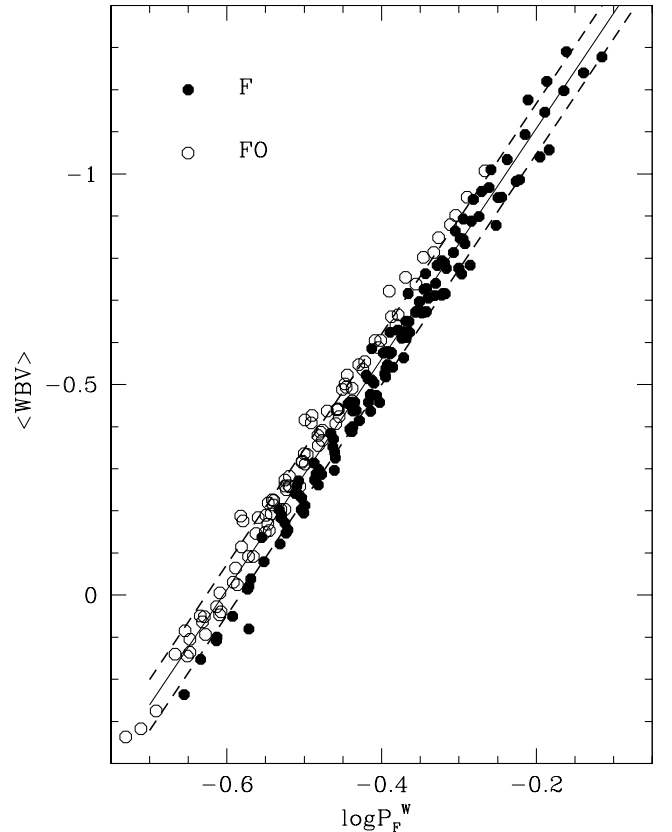$$- 3.350(\pm 0.009) \log T_e + 0.008(\pm 0.001) \log Z, \quad (1)$$

Fig. 2.—PW BV relation for fundamental (*filled circles*) and fundamentalized first overtone (*open circles*) models. The solid line represents the linear regression through the models (see eq. [4a]), while the dashed lines depict the intrinsic dispersion.
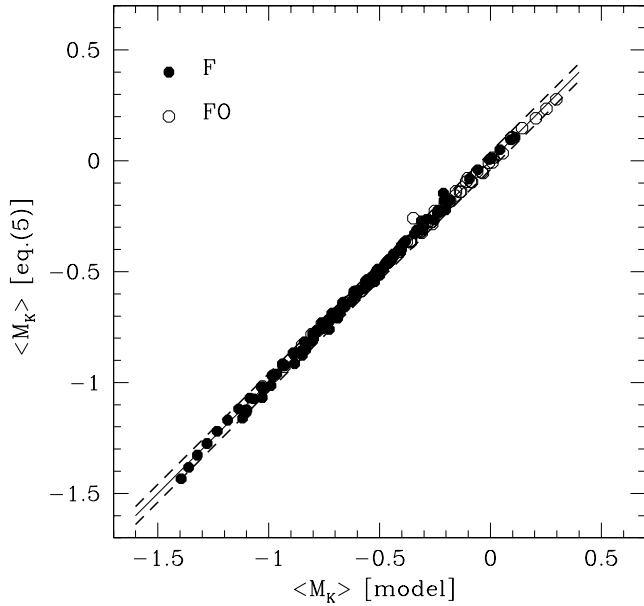

Fig. 1.—Comparison between the computed period of models and the value obtained using eq. (1). The solid line is the 45° line.

FIG. 3.—Comparison between the near-infrared magnitude of models and the value obtained using eq. (5). The solid line is the $45°$ line, while the dashed lines depict the intrinsic dispersion.

in close agreement with earlier results presented by Caputo et al. (1998).

As for the limits of the whole instability strip, namely, the effective temperature of the first-overtone blue edge (FOBE) and of the fundamental red edge (FRE), we find no significative metallicity effect on the FOBE relation at $Z = 0.001$, as given in Paper II, whereas the FRE tends to be slightly redder, for fixed mass and luminosity, when increasing the metal content. However, as already discussed in Paper II, one should also consider that varying the value of the mixing length parameter l/H_p will modify the edges of the pulsation region, shrinking the width of the whole instability strip if increasing the efficiency of convection in the star external layers. In order to study this effect, all the models listed in Table 1, but the case

$Z = 0.0004$, have been recomputed by adopting $l/H_p = 2.0$. The results confirm that the FOBE effective temperature decreases by ~ 100 K, whereas the FRE one increases by ~ 300 K. Moreover, we notice that for the same l/H_p variation the fundamental blue edge changes by 100 K at most, while the first overtone red edge gets hotter by about 200 K.

On this ground, the FOBE and FRE relations at $l/H_p = 1.5$ given in Paper II can be retained over the whole range $Z = 0.0001-0.006$, with a total uncertainty of ± 0.005 and 0.010, respectively, while the effects of a variation of l/H_p from 1.5 to 2.0 on the edges of the instability strip can be quantified as $\Delta \log T_e^{FOBE} = -0.008 \pm 0.003$ and $\Delta \log T_e^{FRE} = 0.021 \pm 0.005$. However, it is of interest to note that with $Z = 0.006$ and $\log L/L_\odot \geq 1.65$ the FO instability strip disappears when $l/H_p = 2.0$ is adopted. Such a result, together with the observational evidence of c-type RR Lyrae stars with such a metal content, seems to suggest that $l/H_p = 2.0$ is a too high value for metal-rich pulsational models.

Concerning the location in the $M_V - \log P$ diagram of the instability strip theoretical edges, taking also into account the above mentioned effects of the mixing-length parameter, a linear regression to the models yields

$$M_V^{FOBE} = -1.19 - 2.23 \log M/M_\odot \\ - 2.54 \log P_{FO} + 0.10(l/H_p - 1.5), \quad (2)$$

$$M_V^{FRE} = 0.12 - 1.88 \log M/M_\odot - 1.96 \log P_F \\ - 0.28(l/H_p - 1.5), \quad (3)$$

with standard deviations of 0.05 and 0.06 mag, respectively.

Before proceeding, let us first recall that, when dealing with pulsating structures, the static magnitudes differ from the measured magnitudes, which are mean quantities (intensity-weighted or magnitude-weighted) averaged over the pulsation cycle. This issue has been discussed in detail in Paper II, and here we wish only to mention that the results at $Z = 0.001$ hold all over the range $Z = 0.0001-0.006$. In particular, we find that the discrepancy between static and mean values is a function of the pulsation amplitude, decreasing from asymmetric
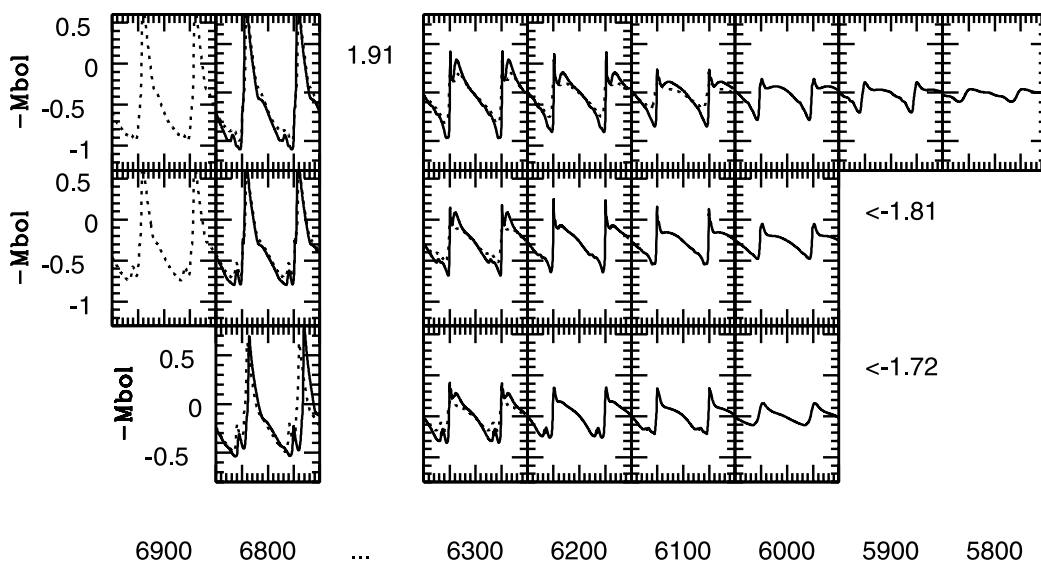

FIG. 4.—Bolometric light curves with $l/H_p = 1.5$ (solid line) and $l/H_p = 2.0$ (dashed line) for a number of F-models with $M = 0.80\ M_\odot$ at varying luminosity and effective temperature.
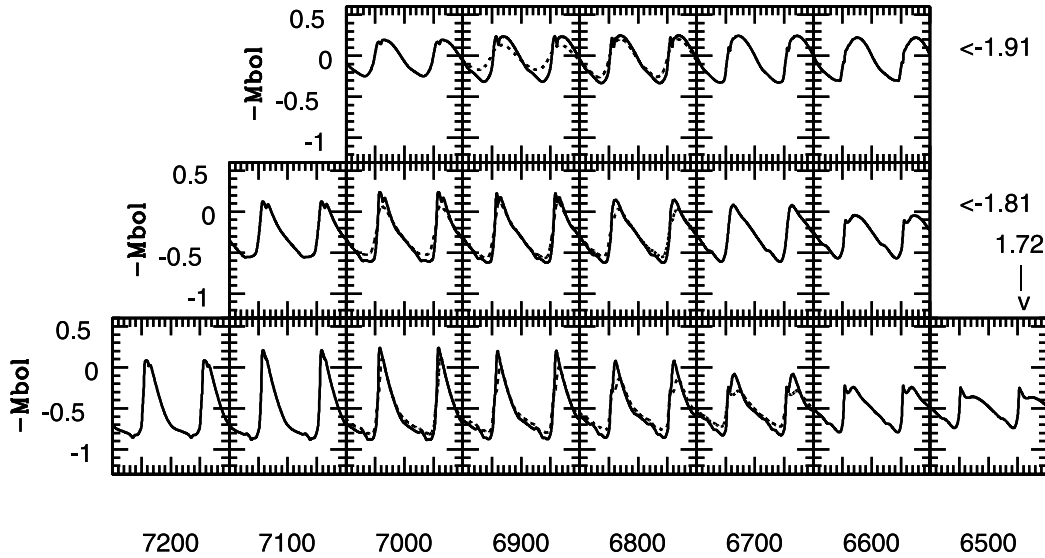
FIG. 5.—Same as in Fig. 4, but for FO models.

to symmetric light curves as well as when passing from optical (BVI) to near-infrared (K) bands, and that intensity-averaged quantities are better representative of static magnitudes and colors. As a whole, each mean magnitude can be corrected for the amplitude effect to get the corresponding static value, or, alternatively, static magnitudes can be directly estimated when the two types of mean values are measured. However, since in the present paper we aim at providing a handy tool for the analysis of observed data, all the following relations will be given for intensity-averaged magnitudes.[4]

The obvious outcome of the period relation (see eq. [1]) into the observational plane is the period-magnitude-color (PMC) relation, where the pulsation period for each given mass is correlated with the pulsator absolute magnitude and color. When using linear pulsating models, this could be made by simply transforming luminosity and effective temperature into absolute magnitude and color, but the result is a *static* PMC relation, which cannot be directly compared to observed variables. On the contrary, our nonlinear approach supplies *mean*

magnitudes and colors. Based on intensity-averaged magnitudes, the linear interpolation through the results (adopting fundamentalized periods for FO models) gives for each adopted metal content Z

$$\log P'_{\rm F} = \log P_{\rm F} + 0.34\langle M_V\rangle + 0.54\log M/M_\odot$$
$$= a(Z) + b(Z)[\langle M_B\rangle - \langle M_V\rangle],$$

where the coefficients $a(Z)$ and $b(Z)$ are listed in Table 2.

As discussed in Paper II, for fixed mass and metal content, the PMC relation defines accurately the properties of individual pulsators within the instability strip, but its use to get distances needs accurate reddening evaluations. However, it is of interest to mention that the magnitude dispersion due to the finite width of the instability strip is rather close to the effect of interstellar extinction. Based on such an evidence, the Wesenheit functions (see Dickens & Saunders 1965) $\mathcal{W}(BV) = V - 3.1(B - V)$, $\mathcal{W}(VI) = V - 2.54(V - I)$, etc., which have been widely used in Cepheid studies (see Madore 1982; Madore & Freedman 1991), can be adopted also for RR Lyrae stars (see Kovacs & Jurcsik 1997; Kovacs & Walker 2001) to provide a reddening-free period-Wesenheit (PW) relation, where also the dispersion

---

[4] The whole set of computed models are available upon request from marcella@na.astro.it.

TABLE 3
EFFECTS OF MIXING-LENGTH PARAMETER l/H_p ON THE PERIOD, COLOR, AND VISUAL AMPLITUDE
OF FUNDAMENTAL MODELS WITH $Z = 0.001$, $0.75\ M_\odot$, AND $\log L/L_\odot = 1.61$

| T_e (K)	($l/H_p = 1.5$)			($l/H_p = 2.0$)		
	P (days)	$\langle M_B\rangle - \langle M_V\rangle$	A_V	P (days)	$\langle M_B\rangle - \langle M_V\rangle$	A_V
6100...............	0.5697	0.423	0.517	Stable	. . .	. . .
6200...............	0.5400	0.405	0.748	Stable	. . .	. . .
6300...............	0.5120	0.385	0.813	0.5109	0.379	0.154
6400...............	0.4859	0.362	0.922	0.4854	0.362	0.548
6500...............	0.4622	0.337	1.162	0.4604	0.342	0.649
6600...............	0.4385	0.310	1.240	0.4384	0.320	0.851
6700...............	0.4170	0.285	1.413	0.4164	0.295	1.074
6800...............	0.3969	0.263	1.544	0.3966	0.271	1.260
6900...............	0.3779	0.244	1.615	0.3780	0.250	1.385
7000...............	FO	. . .	. . .	0.3608	0.231	1.416
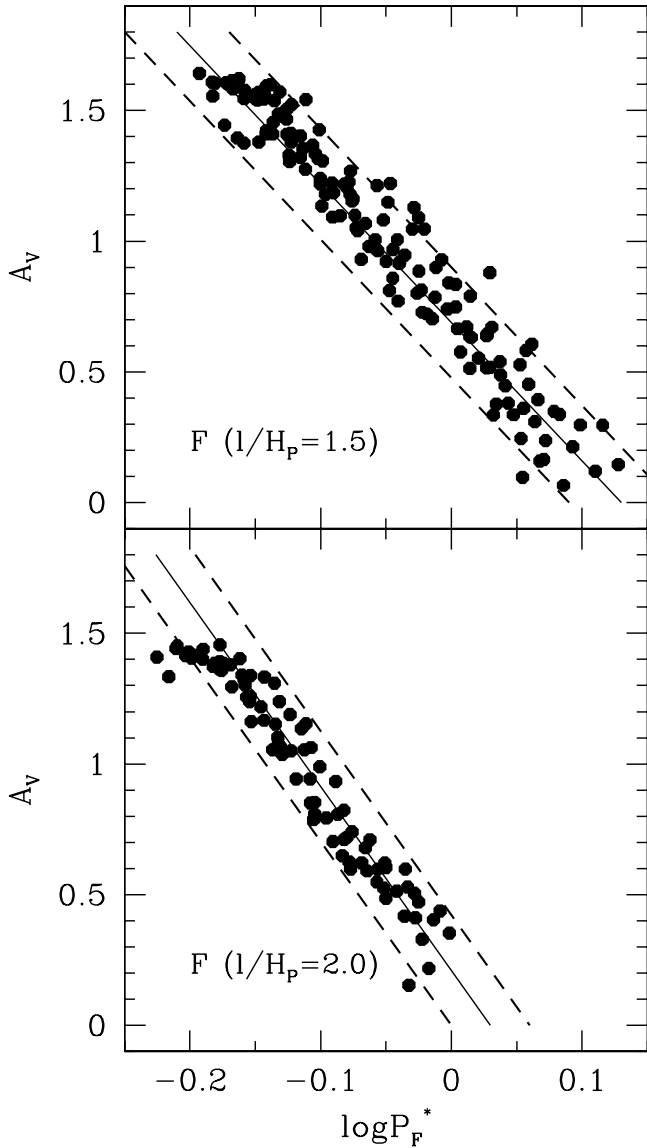
Fig. 6.—Same as Fig. 2, but for the fundamental PMA relations under the two values of the mixing length parameter. The solid lines are the linear regression through the data (see eqs. [6] and [7]), while the dashed lines depict the standard deviation.
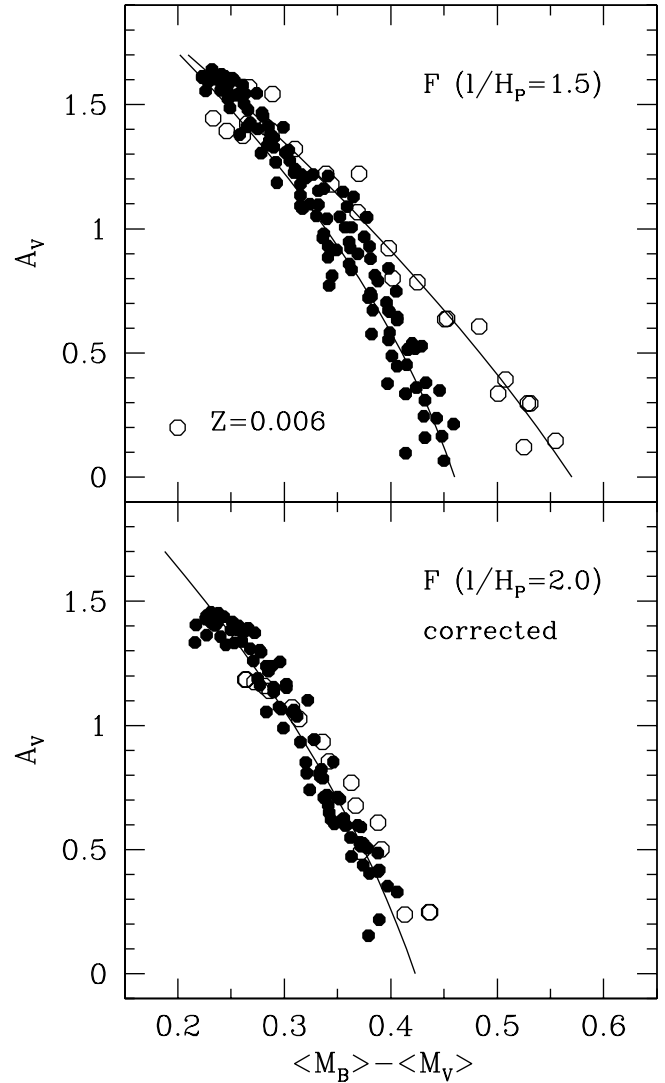

Fig. 7.—*Upper panel:* Visual amplitude A_V as a function of the intensity-weighted $\langle M_B \rangle - \langle M_V \rangle$ color for F pulsators with $l/H_p = 1.5$. The solid lines depict the linear regression through the data (see eqs. [8a] and [8b]). *Lower panel:* As above, but with $l/H_p = 2.0$. The color index is corrected for the metal content and the solid line is the linear regression through the data (see eq. [9]).

of magnitude at a given period is significantly reduced. Before proceeding, let us remark the deep difference between the PMC and PW relations: the former is defined by the intrinsic properties of the variables and cancels the effects of the finite width of the instability strip, while the latter depends on the properties of the interstellar medium and removes any reddening effect, differential or total. Therefore, in the case of variables at the same distance and with the same mass and metal content, the scatter in observed PMC relations, excluding photometric errors, should mainly depend on reddening, whereas the scatter in observed PW relations is a residual effect of the finite width of the strip.

Using $\langle \mathcal{W}(BV) \rangle$ quantities based on intensity-averaged magnitudes, a linear interpolation through F and fundamentalized FO models yields the PW BV relation

$$\langle \mathcal{W}(\mathrm{BV}) \rangle = -1.655(\pm 0.054) - 2.737(\pm 0.027) \log P_{\mathrm{F}}^{\mathcal{W}}, \quad (4a)$$

where

$$\log P_{\mathrm{F}}^{\mathcal{W}} = \log P_{\mathrm{F}} + 0.54 \log M/M_{\odot} + 0.03 \log Z. $$

As shown in Figure 2, the correlation is quite tight, providing a useful way to get the intrinsic distance modulus of variables with known mass and metal content with a formal accuracy of 0.06 mag (*dashed lines*).

As for the $\langle \mathcal{W}(VI) \rangle$ function, the linear interpolation through F and fundamentalized FO models yields

$$\langle \mathcal{W}(VI) \rangle = -1.670(\pm 0.030) - 2.750(\pm 0.013) \log P_{\mathrm{F}}^{\mathcal{W}}, \quad (4b)$$

where

$$\log P_{\mathrm{F}}^{\mathcal{W}} = \log P_{\mathrm{F}} + 0.65 \log M/M_{\odot}. $$

It is of interest to note that RR Lyrae stars observed in the Large Magellanic Cloud yield $\delta \langle \mathcal{W}(VI) \rangle / \delta \log P_{\mathrm{F}} \sim -2.75$ (Soszynski
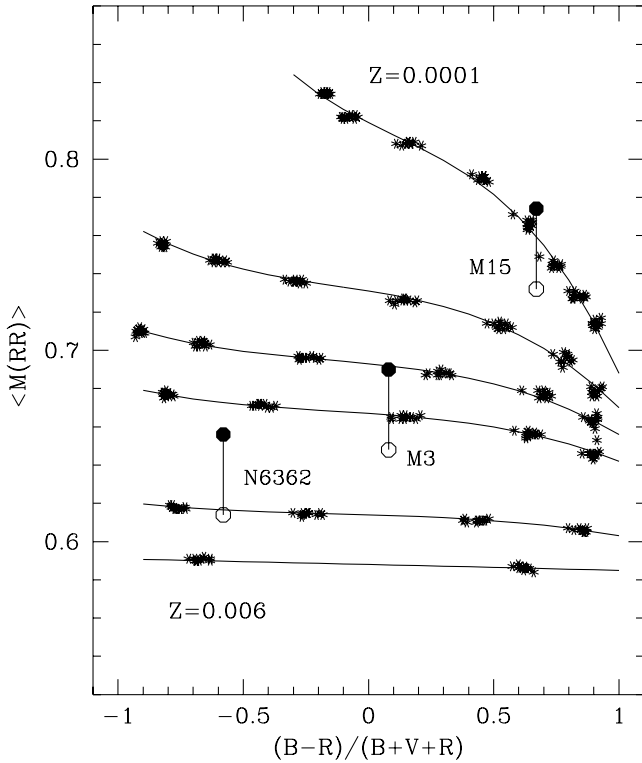
Fig. 8.—Average mass $\langle M(RR) \rangle$ (solar units) of synthetic RR Lyrae pulsators vs. the HB morphology, as inferred from synthetic simulations with metal content $Z = 0.0001$, 0.0003, 0.0006, 0.001, 0.003, and 0.006 (*top to bottom*). The results for some selected globular clusters are reported (see text).

constant mass and metal content, namely, $\delta[\mathcal{W}(BV)]/\delta \log P_F = -2.66(\pm 0.03)$ and $\delta[\mathcal{W}(VI)]/\delta \log P_F = -2.64(\pm 0.02)$.

In matter of distance determinations, let us finally consider the predicted near-infrared period-magnitude (PM_K) relation, which is well known to be a powerful tool to get distances given the quite low dependence of the K-magnitude on interstellar extinction. Adopting again intensity-averaged magnitudes (but in the K-band the difference between intensity-averaged, magnitude-averaged, and static values is quite small because of the reduced pulsation amplitudes), we show in Figure 3 that linear regression through F and fundamentalized FO pulsators provides

$$\langle M_K \rangle = -0.094 - 2.158 \log P_F - 1.436 \log M/M_\odot$$
$$- 0.712 \log L/L_\odot \qquad (5)$$

with a standard deviation of ± 0.04 mag (*dashed lines*).

2.2. Pulsation Amplitudes

Figures 4 and 5 show bolometric light curves with $l/H_p = 1.5$ (*solid line*) and $l/H_p = 2.0$ (*dashed line*) for a number of F and FO models with $M = 0.80 \ M_\odot$ at varying luminosity and effective temperature. In agreement with the results presented in previous papers (Bono & Stellingwerf 1994; Bono et al. 1997), the morphological features of the predicted light curves appear a function of luminosity and effective temperature, thus providing a useful tool to constrain such fundamental intrinsic parameters. In particular, Bono & Stellingwerf (1994) have already discussed that moving toward lower luminosity levels, for a fixed mass, the morphology of the light curve of FO models becomes very similar to that of fundamental pulsators, changing from almost sinusoidal to sawtooth and with a significant increase of the bolometric amplitude. In this context, the use of the Fourier parameters of observed light curves (see, e.g., Kovacs & Walker 2001 and references therein) appears as a promising way to approach the determination of the intrinsic parameters, even though the obvious ultimate goal

et al. 2003), which is the predicted slope at constant mass. Moreover, variables observed in Galactic globular clusters suggest $\delta[\mathcal{W}(BV)]/\delta \log P_F \sim -2.47$ and $\delta[\mathcal{W}(VI)]/\delta \log P_F \sim -2.51$ (see Kovacs & Walker 2001), where $\mathcal{W}(BV)$ and $\mathcal{W}(VI)$ are magnitude-averaged quantities. Also these results appear in reasonable agreement with the predicted slopes we get at roughly

TABLE 4
Selected RR Lyrae–rich Galactic Globular Clusters Listed with Their [Fe/H] Value, HB Type, Apparent Distance Modulus μ_V, and $E(B - V)$ Reddening

NGC/IC	[Fe/H][a]	HB	μ_V (mag)	$E(B - V)$[b] (mag)	RR Lyrae References	$\log Z$ (α/Fe = 0)	$\langle M(RR) \rangle$ ($M/M_\odot$)
4590-M68..................................	−2.43	0.44	15.19	0.05	1	−4.13	0.80
7078-M15..................................	−2.42	0.67	15.37	0.10	2	−4.12	0.77
5466...	−2.22	0.58	16.00	0.00	3	−3.92	0.74
6809-M55..................................	−1.85	0.87	13.87	0.08	4	−3.55	0.69
4499*.......................................	−1.60[a]	0.11	17.09	0.23	5	−3.30	0.70
6934...	−1.59	0.25	16.29	0.10	6	−3.20	0.70
7089-M2....................................	−1.56	0.96	15.49	0.06	7	−3.26	0.66
3201...	−1.56	0.08	14.21	0.23	8	−3.26	0.69
5272-M3....................................	−1.50	0.08	15.12	0.01	9	−3.20	0.69
5904-M5....................................	−1.26	0.31	14.46	0.03	10, 11	−2.96	0.66
1851...	−1.19	−0.36	15.47	0.02	12	−2.89	0.66
6362...	−1.15	−0.58	14.67	0.09	13	−2.85	0.66

Notes.—The reference of the RR Lyrae data is also given. The last two columns give the overall metal content Z, adopting a solar-scaled chemical composition, and the average mass $\langle M(RR) \rangle$ of RR Lyrae stars, as estimated by synthetic horizontal-branch simulations (see text).
[a] From Kraft & Ivans (2003).
[b] $E(B - V)$ reddening from Harris (1996).
[c] [Fe/H] value from Harris (1996).
References.—(1) Walker 1994; (2) Silbermann & Smith 1995; (3) Corwin et al. 1999; (4) Olech et al. 1999; (5) Walker 1996; (6) Kaluzny et al. 2001; (7) Lee & Carney 1999; (8) Piersimoni et al. 2002; (9) Corwin & Carney 2001; (10) Kaluzny et al. 2000; (11) Caputo et al. 1999; (12) Walker & Nemec 1996; (13) A. R. Walker 1999, private communication.
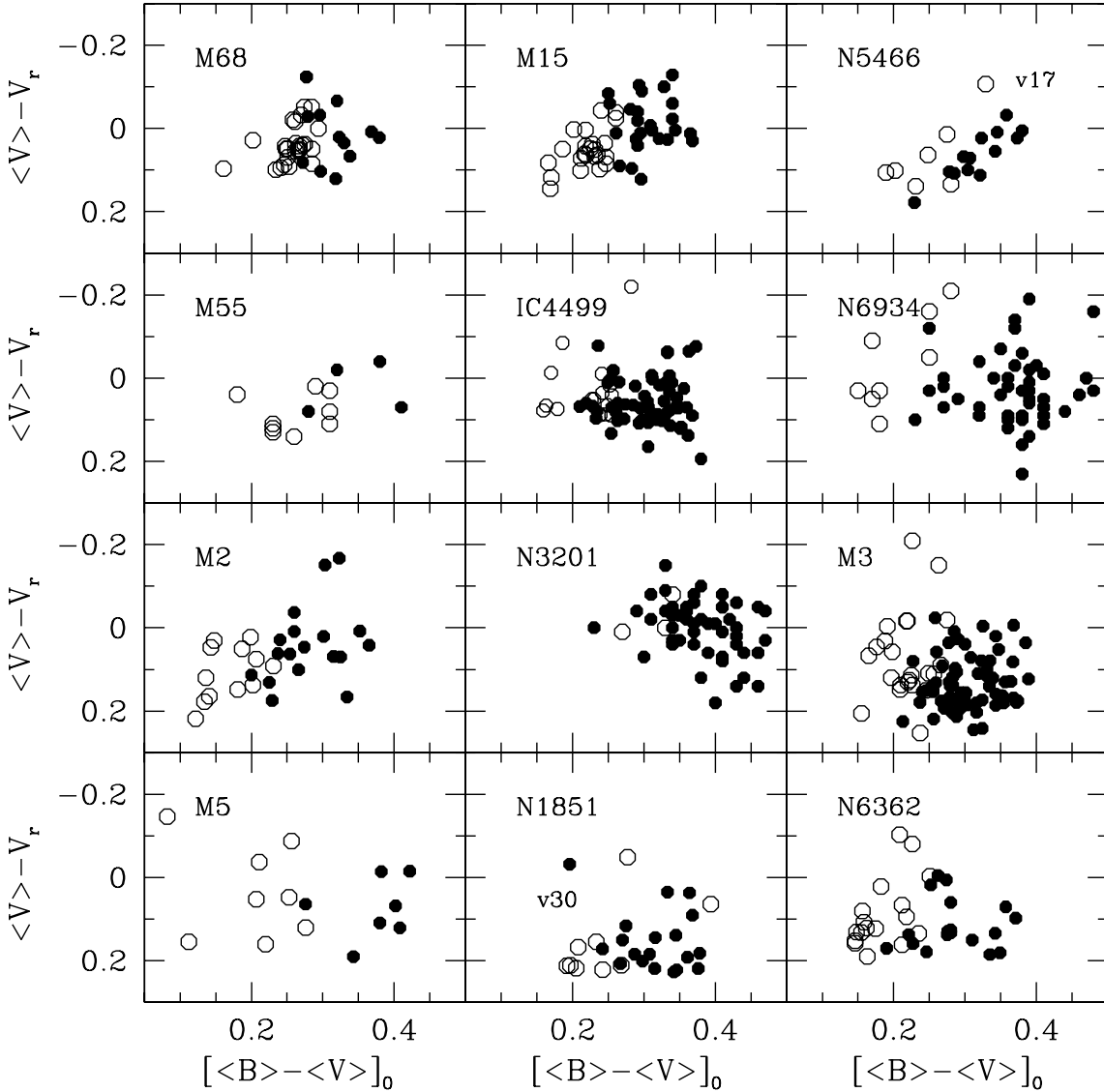
FIG. 9.—Color-magnitude diagram of globular cluster RR$_{ab}$ (*filled circles*) and RR$_c$ (*open circless*) variables, according to intensity-averaged magnitudes scaled to an arbitrary value V_r and $\langle B \rangle - \langle V \rangle$ colors corrected with the $E(B - V)$ values in Table 4.

to take into account all the observed features (e.g., bump, double peak) is the best fit of the whole light curve, as recently presented by Bono et al. (2000, 2002), Castellani et al. (2002), and Di Criscienzo et al. (2003).

Here, as a broad outline of the pulsational behavior, let us consider the quite linear correlation between fundamental bolometric amplitudes and periods (logarithmic scale), for fixed mass and luminosity. However, let us remind that the pulsation amplitudes, while sharing with the periods the property of being sound measurements independent of reddening and distance uncertainties, do significantly depend on the adopted efficiency of the convective transfer. As an example, we list in Table 3 the computed periods, colors, and visual amplitudes for fundamental pulsators with $Z = 0.001$, $0.75\ M_\odot$, $\log L/L_\odot = 1.61$, and $l/H_p = 1.5$ and 2.0. One has that both the period and the color are almost independent of the adopted value for the mixing-length parameter, whereas the amplitude decreases with increasing the efficiency of convection, for fixed effective temperature. Moreover, given the already mentioned effects of the same l/H_p variation on the fundamental red edge (where the amplitude reaches its minimum value) and blue edge (where the

amplitude reaches its maximum value), the $A_V - \log T_e$ slope becomes steeper with increasing the l/H_p value.

As a whole, after transforming all the bolometric light curves into the observational plane, we show in Figure 6 that all over the explored metallicity range the period-magnitude-amplitude (PMA) fundamental relation can be approximated as

$$\log P_F^* = \log P_F + 0.385\langle M_V \rangle \\ + 0.30 \log M/M_\odot = 0.13 - 0.189 A_V \qquad (6)$$

at $l/H_p = 1.5$, and

$$\log P_F^* = \log P_F + 0.385\langle M_V \rangle \\ + 0.35 \log M/M_\odot = 0.03 - 0.142 A_V \qquad (7)$$

at $l/H_p = 2.0$, with standard deviations (*dashed lines*) of 0.04 and 0.03 mag, respectively.

Closing this section devoted to pulsation amplitudes, we notice that increasing the l/H_p value yields smaller amplitudes for fixed BV color (see data in Table 3). This is shown in
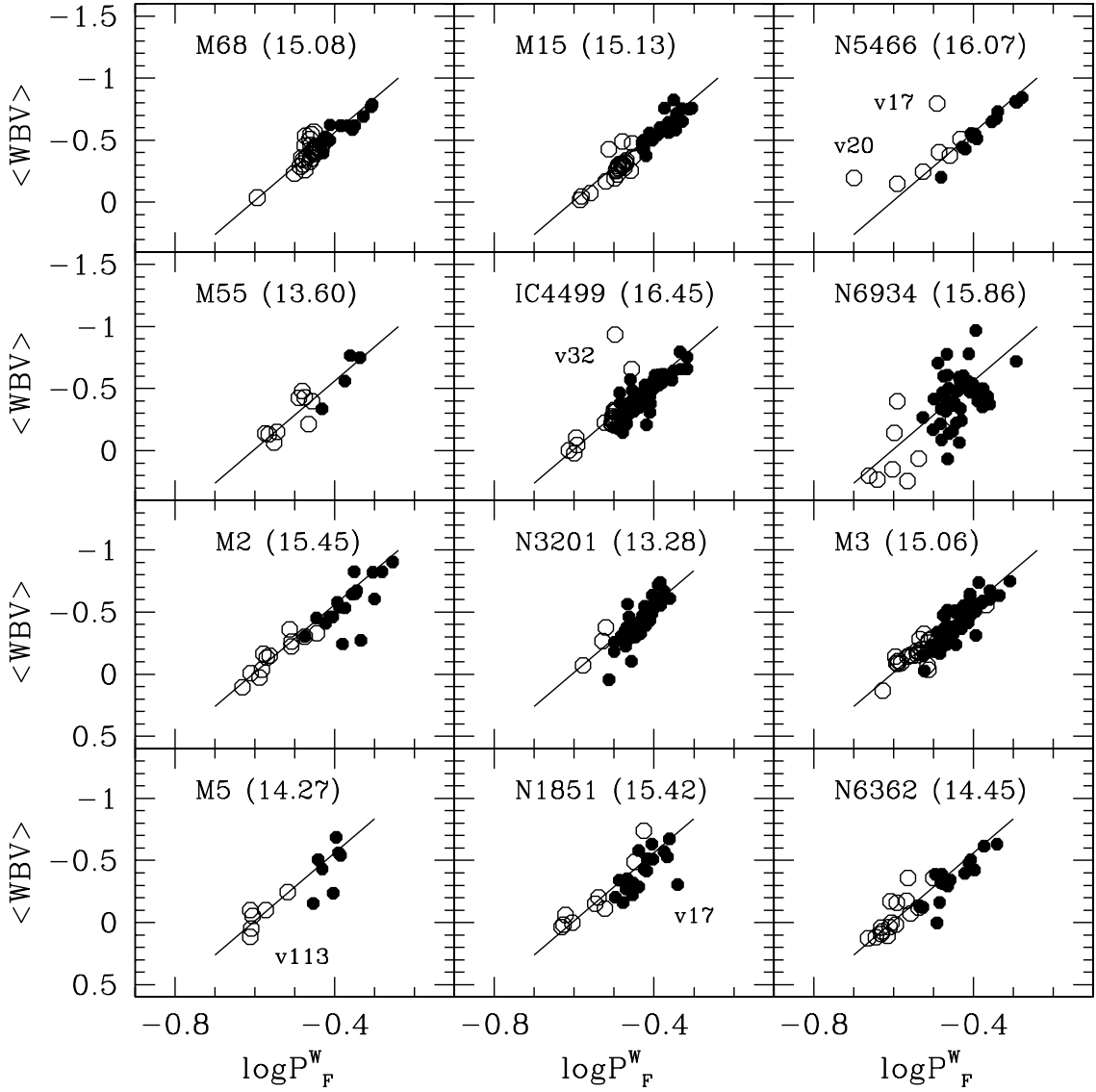
Fig. 10.—Comparison between predicted and observed PW *BV* relations (symbols are as in Fig. 9). The period of c-type variables is fundamentalized and the solid lines depict the predicted behavior at constant mass. The derived intrinsic distance moduli are given in each panel.

TABLE 5

$E(B - V)$ Values and Distance Moduli (in Magnitudes) for the Selected Clusters, as Obtained from the Various Predicted Relations

| NGC/IC (1) | μ_0 (PW *BV*) (2) | $E(B - V)$ | | μ_V | |
		$CA_{1.5}$ (3)	$CA_{2.0}$ (4)	$PMA_{1.5}$ (5)	$PMA_{2.0}$ (6)
4590-M68.................................	15.08 ± 0.07	-0.01 ± 0.02	$+0.04 \pm 0.02$	15.05 ± 0.10	15.24 ± 0.10
7078-M15.................................	15.13 ± 0.08	$+0.02 \pm 0.02$	$+0.07 \pm 0.02$	15.23 ± 0.08	15.41 ± 0.08
5466.......................................	16.07 ± 0.07	-0.01 ± 0.04	$+0.04 \pm 0.03$	16.07 ± 0.09	16.21 ± 0.08
6809-M55.................................	13.60 ± 0.09	$+0.07 \pm 0.04$	$+0.12 \pm 0.04$	13.85 ± 0.05	14.01 ± 0.05
4499.......................................	16.45 ± 0.08	$+0.16 \pm 0.04$	$+0.21 \pm 0.04$	17.01 ± 0.08	17.17 ± 0.08
6934.......................................	15.86 ± 0.12	$+0.10 \pm 0.09$	$+0.15 \pm 0.09$	16.20 ± 0.14	16.35 ± 0.13
7089-M2..................................	15.45 ± 0.11	-0.03 ± 0.03	$+0.02 \pm 0.03$	15.45 ± 0.09	15.63 ± 0.09
3201.......................................	13.28 ± 0.08	$+0.24 \pm 0.04$	$+0.29 \pm 0.04$	14.10 ± 0.13	14.28 ± 0.12
5272-M3..................................	15.06 ± 0.07	-0.03 ± 0.02	$+0.01 \pm 0.02$	15.00 ± 0.08	15.18 ± 0.07
5904-M5..................................	14.27 ± 0.16	$+0.00 \pm 0.03$	$+0.05 \pm 0.03$	14.36 ± 0.09	14.54 ± 0.09
1851.......................................	15.42 ± 0.13	-0.03 ± 0.04	$+0.02 \pm 0.04$	15.38 ± 0.17	15.56 ± 0.17
6362.......................................	14.45 ± 0.09	$+0.01 \pm 0.03$	$+0.06 \pm 0.03$	14.55 ± 0.06	14.71 ± 0.05

Figure 7, where the visual amplitude A_V is plotted as a function of the intensity-weighted $\langle M_B \rangle - \langle M_V \rangle$ color for F pulsators with $l/H_p = 1.5$ (*upper panel*) and $l/H_p = 2.0$ (*lower panel*). At variance with the results derived with static colors, here one derives that the amplitude-color correlation is not strictly linear as a consequence of the fact that at larger amplitudes the intensity-averaged color becomes bluer than the static one (see Paper II). As a whole, in the explored range of mass and luminosity, all the results with $l/H_p = 1.5$ and $Z \leq 0.001$ suggest the color-amplitude (CA) relation

$$\langle M_B \rangle - \langle M_V \rangle = 0.469 - 0.077 A_V - 0.044 A_V^2, \quad (8a)$$

with a standard deviation of 0.04 mag, while at $Z = 0.006$ we get

$$\langle M_B \rangle - \langle M_V \rangle = 0.568 - 0.156 A_V - 0.033 A_V^2, \quad (8b)$$

with a standard deviation of 0.02 mag. As for the case $l/H_p = 2.0$, the regression through all the models yields

$$\langle M_B \rangle - \langle M_V \rangle = 0.465 - 0.079 A_V$$
$$- 0.035 A_V^2 + 0.014 \log Z \quad (9)$$

with a standard deviation of 0.03 mag.

3. COMPARISON WITH OBSERVED RR LYRAE STARS

As discussed in Paper II, synthetic horizontal-branch (SHB) simulations based on HB evolutionary tracks and pulsational constraints provide reliable information on the HB morphology (as given by the ratio $(B - R)/(B + V + R)$, where B, V, and R represent the numbers of blue, variable, and red HB stars), as well as on the "evolutionary" FOBE and FRE of the synthetic pulsator distribution, for each given metal content and average mass of HB stars. It follows that, if the metal content and HB morphology are known, one can evaluate the average mass of RR Lyrae stars to be inserted into the mass-dependent relations presented in the previous section. As an example, we show in Figure 8 the correlation between the HB morphology and the average mass $\langle M(\mathrm{RR}) \rangle$ (solar units) of RR Lyrae stars, as derived from synthetic simulations based on HB models with $Z = 0.0001$, 0.0003, 0.0006, 0.001, 0.003, and 0.006 (S. Cassisi et al. 2004, in preparation [Paper IV]). In this figure, the large circles depict three selected clusters (M15, M3, and NGC 6362), which are plotted according to their observed HB type and measured [Fe/H] value (see Table 4), under the assumption of solar-scaled ($[\alpha/\mathrm{Fe}] = 0$; *filled circles*) or α-enriched ($[\alpha/\mathrm{Fe}] \sim 0.5$; *open circles*) chemical compositions.

In view of the somehow different HB models published in the recent literature, the present paper was mainly intended to illustrate the results of pulsation models, leaving the mass as a free parameter and reserving to Paper IV the connection to stellar evolution theory and the construction of synthetic relations based also on the evolutionary times. Nevertheless, in order to check the internal consistency of the pulsational framework, as well as its appropriateness at the various metal contents, let us rely on the results plotted in Figure 8 to compare the predictions presented in the previous section with observed data of RR Lyrae–rich globular clusters with available B, V, A_V measurements. The selected clusters are listed in Table 4, together with their [Fe/H] value (Kraft & Ivans 2003), HB type, apparent distance modulus μ_V and $E(B - V)$ reddening (from Harris 1996), and the source of RR Lyrae data. The last two
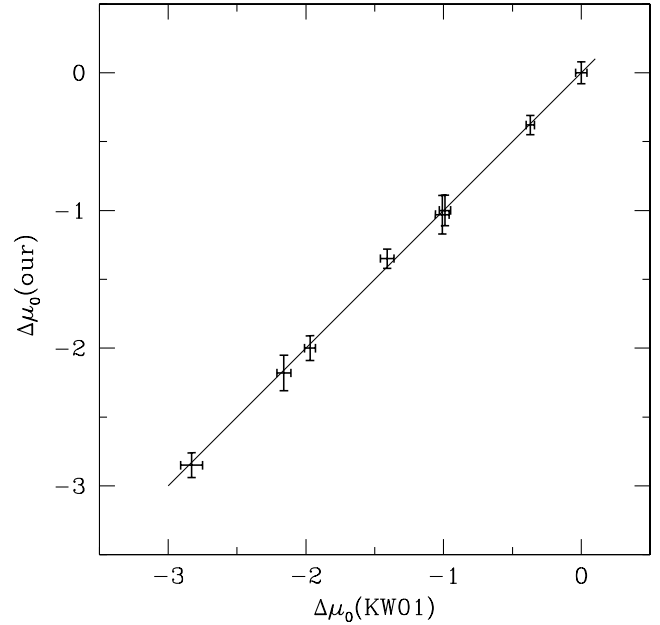

Fig. 11.—Comparison between our predicted intrinsic distance moduli and those derived by Kovacs & Walker (2001). The values are scaled to the intrinsic distance modulus of IC 4499.

columns in Table 4 give the overall metal content Z for a solar-scaled chemical composition (i.e., $\log Z = [\mathrm{Fe/H}] - 1.70$) and the average mass of the RR Lyrae stars, as inferred from the results plotted in Figure 8.

A general overview of data is shown in Figure 9, where the variables are plotted in the color-magnitude diagram according to intensity-averaged magnitudes, scaled to an arbitrary value V_r, and intrinsic colors, as derived using $E(B - V)$ values in Table 4. Filled and open circles are RR_{ab} and RR_c stars, as given by the authors, and some outliers with respect to the average distribution are marked.

Starting with the PW relation, which is independent of the adopted mixing-length parameter, we show in Figure 10 the comparison between observed $\langle \mathcal{W}(BV) \rangle$ quantities (the symbols are as in Fig. 9) and the predicted relation (see eq. [4a]). For each cluster, $\log P_F^{\mathcal{W}}$ is evaluated according to the mass and metal content listed in Table 4, while the solid lines drawn in the panels depict the predicted behavior at constant mass and metallicity, as reasonably adopted for RR Lyrae stars in a given globular cluster. In this reddening-free diagram, only the NGC 6934 variables exhibit a considerable scatter, suggesting that observational errors are possibly occurring in the data. For the remaining clusters, with the exception of very few outliers, the observed data fit quite well the predicted slope, allowing us to derive the intrinsic distance moduli labeled in the various panels of the figure and listed in column (2) of Table 5. It is quite interesting to note that these theoretical distance moduli appear in agreement with previous empirical determinations. This is shown in Figure 11, where the relative values with respect to IC 4499, taken as reference cluster, are plotted versus the evaluations given by Kovacs & Walker (2001).

Before proceeding with further comparison between theory and observation, one has to notice that all other predictions depend on the adopted mixing-length parameter. One may attempt to have a look on such an issue making use of the predicted color-amplitude fundamental relation, which is independent of the pulsator mass and of the reddening values
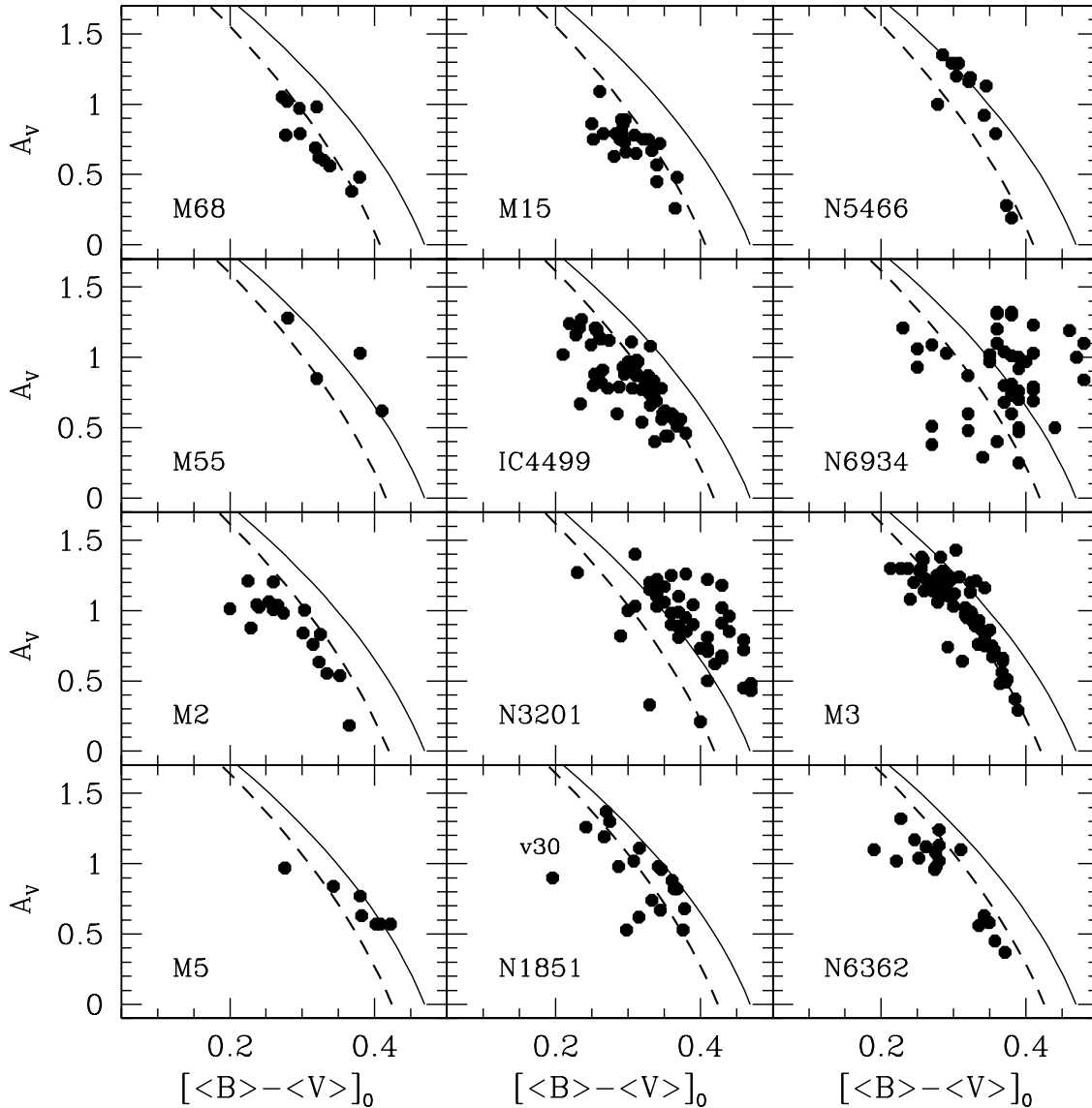
Fig. 12.—Visual amplitude of cluster ab-type variables vs. the intrinsic $[\langle B \rangle - \langle V \rangle]_0$ color, compared with the predicted relation at $l/H_p = 1.5$ (*solid line*) and $l/H_p = 2.0$ (*dashed line*).

given in Table 4. Figure 12 shows the visual amplitude of RR$_{ab}$ stars in our sample versus the intrinsic color $[\langle B \rangle - \langle V \rangle]_0$, in comparison with the theoretical relations at $l/H_p = 1.5$ (eq. [8a]; *solid line*) and 2.0 (eq. [9]; *dashed line*). Disregarding M5 and M55, for the scarcity of data, and NGC 6934, for the well-known significantly inhomogeneous reddening, one finds that all the remaining clusters seem to exclude $l/H_p = 1.5$, except NGC 3201 and NGC 5466. On this basis, even if tempted to take $l/H_p = 2.0$ as the preferred choice, we keep both the alternative values and we use equations (8a) and (9) to derive the $E(B - V)$ values listed in columns (3) and (4) of Table 5.

Adopting again the mass values in Table 4, we use now the predicted PMA relation (see eqs. [6] and [7]) for fundamental pulsators to estimate the apparent distance modulus. Figure 13 shows the RR$_{ab}$ variables plotted in the $A_V - \log P_F^*$ plane, in comparison with the predicted behavior at constant mass and $l/H_p = 1.5$ (*solid line*). The derived apparent distance moduli are labeled in the various panels and listed in column (5) in Table 5, while the following column in the same table gives the results of a similar comparison, but with $l/H_p = 2.0$.

Finally, we show in Figure 14 the comparison between the observed distribution of RR Lyrae stars in the $\langle V \rangle - \log P$ plane and the predicted edges of the instability strip, as estimated inserting the mass values in Table 4 into equations (2) and (3). We start fitting the predicted FOBE at $l/H_p = 1.5$ (*solid line at the left*) to the observed distribution of c-type variables under the condition that no c-type variables are left in the hot stable region. As shown in Figure 14, the apparent distance modulus derived in such a way (the values are labeled in the panels and listed in col. [2] of Table 6) yields a quite good agreement between the ab-type distribution and the predicted FRE (*solid line at the right*), except for M68, M15, NGC 5466, M55, and NGC 3201. For these clusters, the observed period distribution of ab-type variables would suggest a red edge as depicted by the dashed line. In other words, under the assumption that the whole instability strip is populated, for these clusters the right value of the distance modulus to fit the observed distribution of ab-type variables is smaller by ~ 0.15 mag than the value derived from the FOBE-procedure (see col. [3] in Table 6).

Let us now repeat the comparison, but with $l/H_p = 2.0$. Since the predicted FOBE becomes fainter by ~ 0.05 mag, the
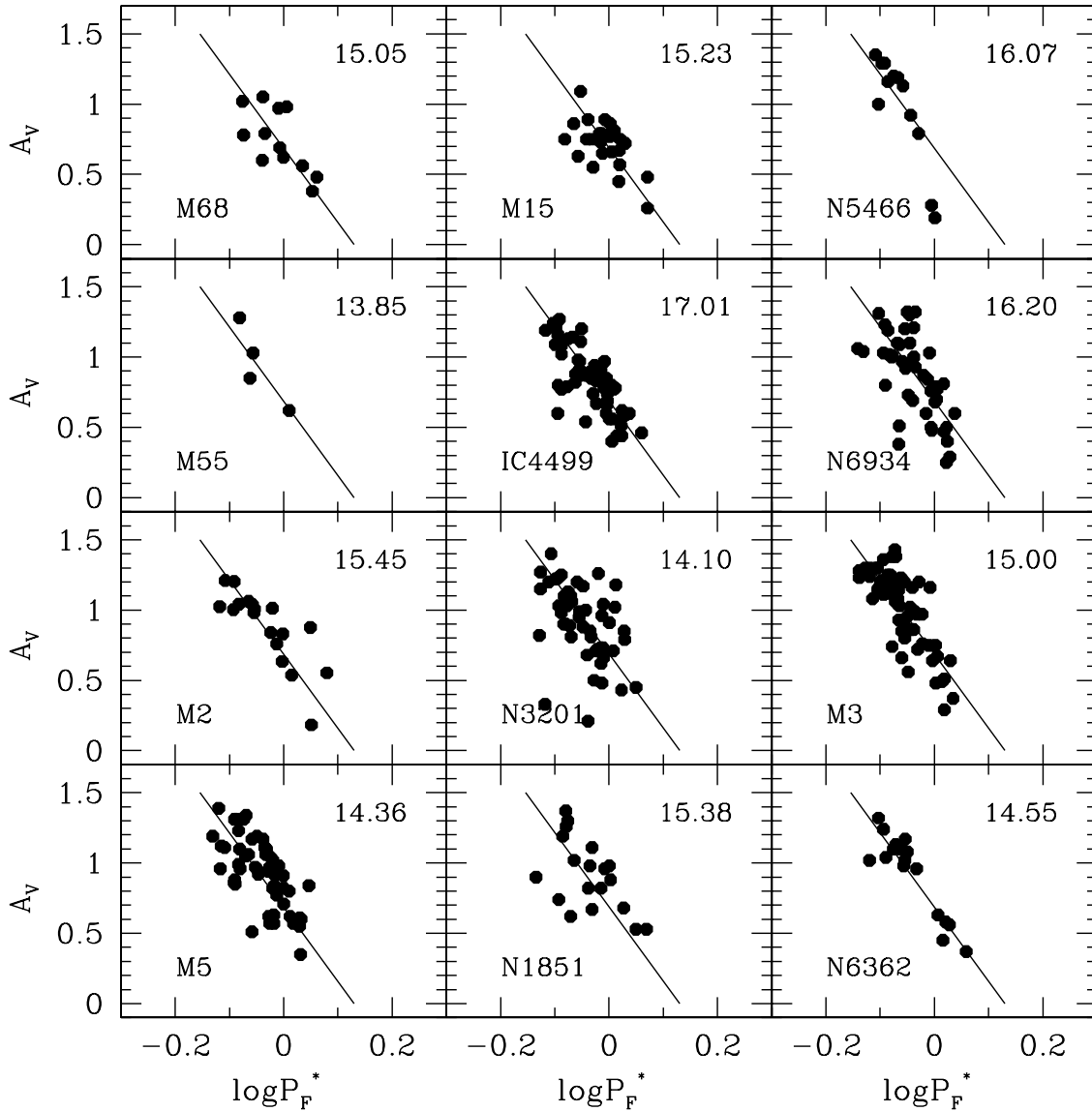
Fig. 13.—Same as Fig. 11, but for the PMA relation of fundamental pulsators at $l/H_p = 1.5$. The solid lines are the predicted slope at constant mass. The derived apparent distance moduli are given in each panel.

right distance modulus to fit the observed distribution of c-type variables decreases by the same quantity. However, at the same time the predicted FRE becomes brighter by ~ 0.14 mag and, as shown in Figure 15, for some clusters several ab-type variables would have longer periods than the predicted FRE. Specifically, for IC 4499, NGC 6934, M2, M3, M5, NGC 1851, and NGC 6362 the comparison of the predicted FRE to the observed red edge (*dashed line*) would yield now a distance modulus which is larger by ~ 0.10 mag than the one derived from the FOBE-procedure.

We summarize in Table 6 the distance moduli inferred from the $M_V - \log P$ distribution. One can conclude that the assumption $l/H_p = 1.5$ yields rather discordant results for M68, M15, NGC 5466, M55, and NGC 3201, where a quite close agreement is present with $l/H_p = 2.0$. On the other hand, the assumption $l/H_p = 2.0$ yields rather discordant results for the remaining clusters (IC 4499, NGC 6934, M2, M3, M5, NGC 1851, and NGC 6362), for which a better agreement is reached with $l/H_p = 1.5$. In summary, present results would suggest that the assumption of a constant mixing-length parameter should be revisited.

However, recent evolutionary studies seem to exclude any trend of the l/H_p ratio with the metal content (see Palmieri et al. 2002, Lastennet et al. 2003). Conversely, specific tests aiming at fitting the light curves of observed pulsators (both RR Lyrae stars and Classic Cepheids) with modeled curves have shown that first overtone (hotter pulsators) light curves are well reproduced with $l/H_p = 1.5$, whereas in the case of fundamental variables (cooler pulsators) a value $l/H_p \geq 1.8$ is needed in order to properly reproduce both the amplitude and the morphology of observed curves (see Bono et al. 2000, 2002; Castellani et al. 2002; Di Criscienzo et al. 2003).

According to such a suggestion of a mixing-length parameter increasing from the FOBE to the FRE (see also Paper II), we eventually list in column (6) of Table 6 the apparent distance modulus of each cluster, as given by the weighted mean over the values listed in column (6) of Table 5 and in columns (2) and (5) of Table 6. As shown in Figure 16, the comparison between our relative distance moduli and those obtained by Kovacs & Walker (2001) on the basis of empirical relations based on Fourier parameters of the light curves discloses again a quite good agreement. As for the absolute values, let us remark that
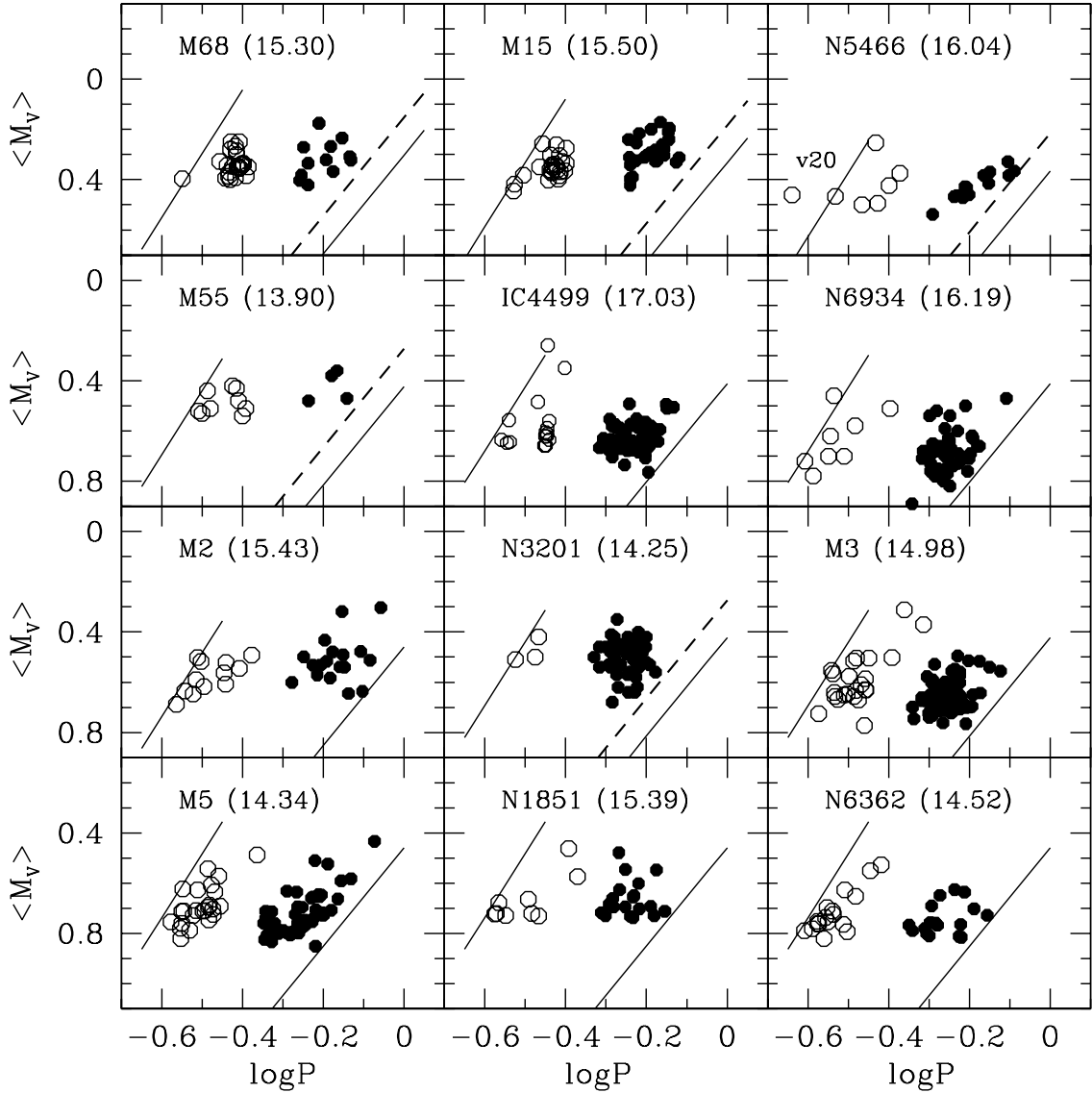
Fig. 14.—Observed distribution of RR Lyrae stars in the $M_V - \log P$ plane in comparison with the predicted edges of the instability strip at $l/H_p = 1.5$ (*solid lines*). The distance modulus labeled in each panel is obtained by fitting the observed distribution of c-type variables (*open symbols*) to the predicted FOBE. The dashed lines depict the observed limit of ab-type variables under the hypothesis of a well-populated instability strip.

TABLE 6

FOBE and FRE Distance Moduli (in Magnitudes) for the Selected Clusters, as Obtained with Different Assumptions on the Mixing-Length Parameter

|	μ_V				
NGC Cluster (1)	FOBE$_{1.5}$ (2)	FRE$_{1.5}$ (3)	FOBE$_{2.0}$ (4)	FRE$_{2.0}$ (5)	$\langle \mu_V \rangle^a$ (6)
4590-M68...	15.30 ± 0.07	15.15 ± 0.08	15.25 ± 0.07	15.25 ± 0.08	15.27 ± 0.05
7078-M15...	15.50 ± 0.07	15.35 ± 0.08	15.45 ± 0.07	15.45 ± 0.08	15.46 ± 0.04
5466...	16.04 ± 0.07	14.99 ± 0.08	15.99 ± 0.07	15.99 ± 0.08	16.08 ± 0.04
6809-M55...	13.90 ± 0.07	13.75 ± 0.08	13.85 ± 0.07	13.85 ± 0.08	13.95 ± 0.04
4499...	17.03 ± 0.07	17.03 ± 0.08	16.98 ± 0.07	17.08 ± 0.08	17.09 ± 0.04
6934...	16.19 ± 0.07	16.19 ± 0.08	16.14 ± 0.07	16.24 ± 0.08	16.23 ± 0.05
7089-M2...	15.43 ± 0.07	15.43 ± 0.08	15.38 ± 0.07	15.48 ± 0.08	15.50 ± 0.04
3201...	14.25 ± 0.07	14.10 ± 0.08	14.20 ± 0.07	14.20 ± 0.08	14.24 ± 0.05
5272-M3...	14.98 ± 0.07	14.98 ± 0.08	14.93 ± 0.07	15.03 ± 0.08	15.07 ± 0.04
5904-M5...	14.34 ± 0.07	14.34 ± 0.08	14.29 ± 0.07	14.39 ± 0.08	14.41 ± 0.04
1851...	15.39 ± 0.07	15.39 ± 0.08	15.34 ± 0.07	15.44 ± 0.08	15.42 ± 0.05
6362...	14.52 ± 0.07	14.52 ± 0.08	14.47 ± 0.07	14.57 ± 0.08	14.63 ± 0.04

^{a} Adopted average distance modulus.
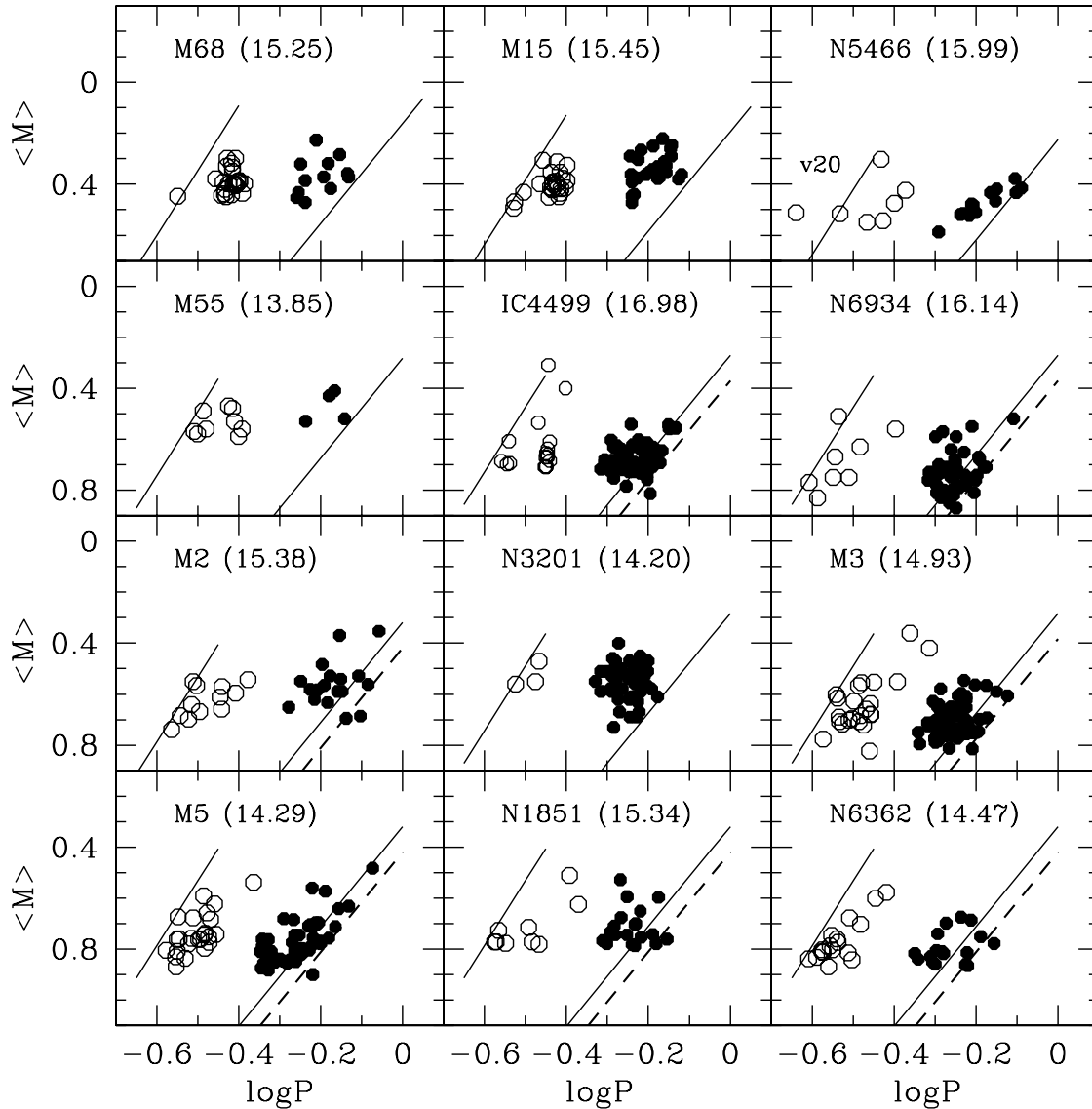
FIG. 15.—Same as Fig. 14, but adopting $l/H_p = 2.0$.

the distance moduli reported in Table 6 hold adopting the SHB simulations depicted in Figure 8, CGKa and CGKb bolometric corrections, as well as solar-scaled chemical compositions. Concerning this last point, the same Figure 8 shows the decrease of the RR Lyrae average mass ($\Delta \log M \sim -0.03$) if adopting α-enriched ($[\alpha/Fe] \sim 0.5$) chemical mixtures, namely, $\Delta \log Z \sim 0.38$ for any fixed [Fe/H] value. As a consequence, the values listed in Tables 5 and 6 should be decreased by $\Delta\mu_V$(FOBE/FRE) ~ -0.06 mag, $\Delta\mu_V$(PMA) ~ -0.03 mag, and $\Delta\mu_0$(PW) ~ -0.01 mag.

4. CONCLUSIONS

It is widely recognized that the main tool for interpreting the observed properties of HB stars is based on the constraints predicted by synthetic horizontal branches. Such synthetic simulations require updated evolutionary models and, in order to extend the analysis to RR Lyrae variables, trustworthy pulsating models computed with the same updated input physics (e.g. opacity tables) and assumptions on free parameters (e.g., l/H_p).

In Paper II we have shown that such an approach yields a pulsational route to accurate distance determinations for the

globular cluster M3. The main purpose of the present paper is to complete the pulsational study, providing theoretical relations for the analysis of RR Lyrae stars with metal content $Z = 0.0001–0.006$.

The comparison with variables in selected globular clusters shows that the slope of the predicted relations is in reasonable agreement with the observed distributions, allowing us to proceed in determining the true distance modulus, as well as reddening and apparent distance moduli under two assumptions for the mixing-length parameter. Adopting recent suggestions that the value of such a parameter may increase from the blue to the red edge of the pulsation region, we obtain a close agreement among the distance moduli inferred by the various approaches, supporting the self-consistency of the pulsational scenario. Moreover, we show that the relative distance moduli derived in this paper, both apparent and intrinsic, match well those inferred by empirical relations (see Kovacs & Walker 2001).

As for the absolute values, we emphasize that they depend on the adopted evolutionary mass of the variables, which in turn mainly depends on the adopted ratio between α and heavy elements, decreasing when passing from solar-scaled to
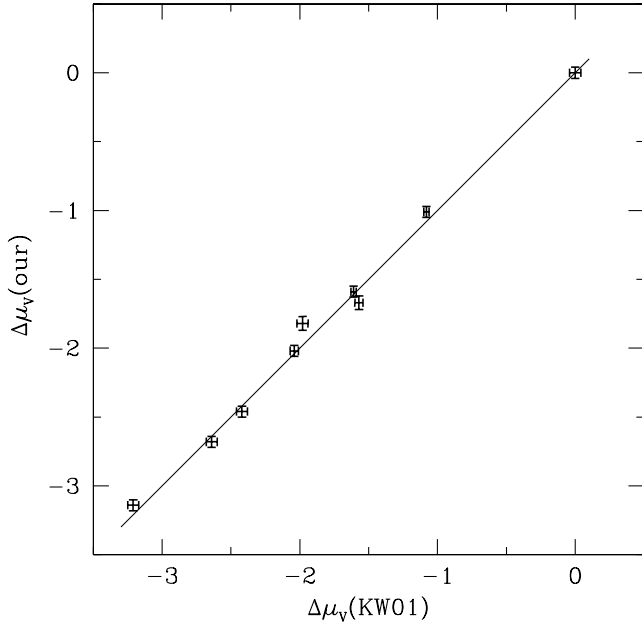
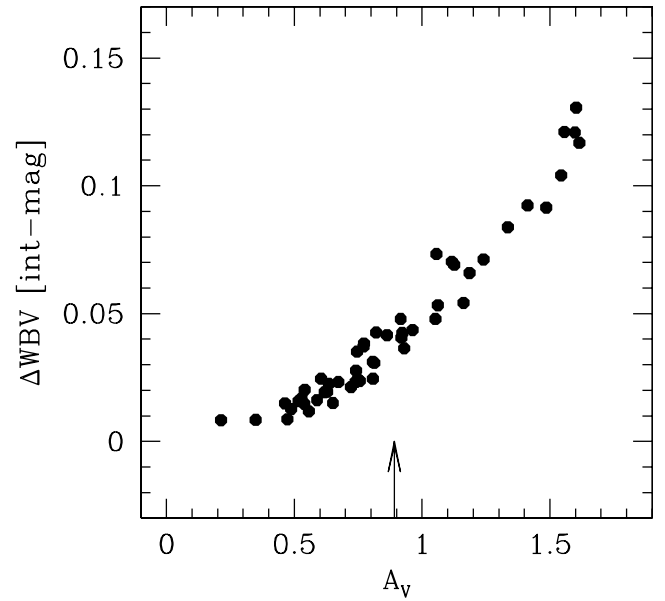Fig. 16.—Same as Fig. 11, but with the apparent distance moduli.

Fig. 17.—Difference between intensity-weighted and magnitude-weighted Wesenheit functions vs. the visual amplitude, as inferred by the pulsating models. The arrow depicts the observed visual amplitude of RR Lyr.

α-enriched mixtures, for fixed [Fe/H]. On this issue, it is worth mentioning that empirical results suggest $[\alpha/\mathrm{Fe}] \sim 0.3$ (Carney 1996; Lee & Carney 2002) and that such a value is consistent with the global features of color-magnitude diagrams (Caputo & Cassisi 2002). Finally, let us remind that different bolometric corrections are still used by the various researchers (see Paper II) and that the current discrepancy of ~ 0.05–0.06 mag requires some firm solutions.

However, it is of interest to note that a previous comparison (see Bono et al. 2003) between pulsational prescriptions and observed V and K magnitudes of the prototype variable RR Lyr yields a "pulsational" parallax quite close with the *HST* direct measurement. Using here magnitude-averaged (B) and (V) data, as listed in Bono et al. (2003), we get that the observed magnitude-averaged Wesenheit function of RR Lyr is $(BV) = 6.634$ mag. In order to transform this figure into the intensity-weighted value, we use the predicted correlation plotted in Figure 17, where $\Delta \mathcal{W}(BV) = \langle(BV)\rangle - [\mathcal{W}(BV)]$ and A_V is the visual amplitude. With $A_V(\mathrm{RR\ Lyr}) = 0.89$ mag, one derives $\langle \mathcal{W}(BV)\rangle = 6.68 \pm 0.02$ mag, where the error is due to the intrinsic spread in Figure 17. Adopting for RR Lyr, $\log P = -0.2466$ and $[\mathrm{Fe/H}] = -1.39$ (see Bono et al. 2003 for references), and assuming a mass in the range of 0.66 (as

adopted in M5 with $[\mathrm{Fe/H}] = -1.29$) to 0.69 $M_\odot$ (as adopted in M3, with $[\mathrm{Fe/H}] = -1.50$), equation (4a) gives the absolute value $\langle \mathcal{W}(BV)\rangle = -0.47 \pm 0.05$ mag, which means an intrinsic distance modulus $\mu_0 = 7.15 \pm 0.06$ mag and a "pulsational" parallax $\pi_\mathrm{puls} = 3.72 \pm 0.10$ mas, which is consistent with the *HST* geometric measurement $\pi_\mathrm{trig} = 3.82 \pm 0.20$ mas.

REFERENCES

Benedict, G. F., et al. 2002, AJ, 123, 473
Bono, G., Caputo, F., Castellani, V., & Marconi, M. 1997, A&AS, 121, 327
Bono, G., Caputo, F., Castellani, V., Marconi, M, & Storm, J. 2001, MNRAS, 326, 1183
Bono, G., Caputo, F., Castellani, V., Marconi, M, Storm, J., & Degl'Innocenti, S. 2003, MNRAS, 344, 1097
Bono, G., Castellani, V., & Marconi, M. 2000, ApJ, 532, L129
———. 2002, ApJ, 565, L83
Bono, G., & Stellingwerf, R. F. 1994, ApJS, 93, 233
Cacciari, C. 2003, in ASP Conf. Ser. 296, New Horizons in Globular Cluster Astronomy, ed. G. Piotto et al. (San Francisco: ASP), 329
Caputo, F., & Cassisi, S. 2002, MNRAS, 333, 825
Caputo, F., Castellani, V., Marconi, M., & Ripepi, V. 1999, MNRAS, 306, 815
Caputo, F., Santolamazza, P., & Marconi, M. 1998, MNRAS, 293, 364
Carney, B. W. 1996, PASP, 108, 900
Carretta, E., Gratton, R. G., Clementini, G., Fusi Pecci, F. 2000, ApJ, 533

Cassisi, S., Castellani, M., Caputo, F., & Castellani, V. 2004, preprint (astro-ph/0407256) (Paper IV)
Castellani, M., Caputo, F., & Castellani, V. 2003, A&A, 410, 871 (Paper I)
Castellani, V., Degl'Innocenti, S., & Marconi, M. 2002, in ASP Conf. Ser. 265, Omega Centauri: A Unique Window into Astrophysics, ed. F. van Leeuwen, J. P. Hughes, & G. Piotto (San Francisco: ASP), 193
Castelli, F., Gratton, R. G., & Kurucz, R. L. 1997a, A&A, 318, 841 (CGKa)
———. 1997b, A&A, 324, 432 (CGKb)
Clement, C. M., et al. 2001, AJ, 122, 2587
Corwin, T. M., & Carney, B. W. 2001, AJ, 122, 3183
Corwin, T. M., Carney, B. W., & Nifong, B. C. 1999, AJ, 118, 2875
Dickens, R. J., & Saunders, J. 1965, Royal Obs. Bull., 101, 101
Di Criscienzo, M. 2002, Ph.D. thesis, Univ. Naples
Di Criscienzo, M., Marconi, M., & Caputo, F. 2003, Mem. Soc. Astron. Italiana, 75, 190
Harris, W. E. 1996, AJ, 112, 1487

Kaluzny, J., Olech, A., Thompson, I. B., Pych, W., Krzeminski, W., & Shwarzenberg-Czerny, A. 2000, A&AS, 143, 215
Kovacs, G., & Jurcsik, J. 1997, A&A, 322, 218
Kovacs, G., & Walker, A. R. 2001, A&A, 374, 264
Kraft, R. P., & Ivans, I.I. 2003, PASP, 115, 143
Lastennet, E., Fernandes, J., Valls-Gabaud, D., & Oblak, E. 2003, A&A, 409, 611
Lee, J. W., & Carney, B. W. 1999, AJ, 117, 2868
———. 2002, AJ, 124, 1511
Madore, B. F. 1982, ApJ, 253, 575
Madore, B. F., & Freedman, W. L. 1991, PASP, 103, 933
Marconi, M., Caputo, F., Di Criscienzo, M., & Castellani, M. 2003, ApJ, 596, 299 (Paper II)

Olech, A., Kaluzny, J., Thompson, I. B., Pych, W., Krzeminski, W., & Shwarzenberg-Czerny, A. 1999, AJ, 118, 442
Palmieri, R., Piotto, G., Saviane, I., Girardi, I., & Castellani, V. 2002, A&A, 392, 115
Piersimoni, A., Bono, G., & Ripepi, V. 2002, AJ, 124, 1528
Silbermann, N. A., & Smith, H. A. 1995, AJ, 110, 704
Soszynski, I., et al. 2003, Acta Astron., 53, 93
Walker, A. R. 1994, AJ, 108, 555
———. 1998, AJ, 116, 220
Walker, A. R. & Nemec, J. M. 1996, AJ, 112, 2026